

(Scientific Note)

# The Use of Neural Networks in Radiometric Studies of Land Surface Parameters

YUEI-AN LIOU\*, YU-CHANG TZENG\*\*, AND KUN-SHAN CHEN\*

\*Center for Space and Remote Sensing Research  
National Central University

Chungli, Taiwan, R.O.C.

\*\*Department of Electronic Engineering  
National Lien-Ho College of Technology and Commerce  
Miaoli, Taiwan, R.O.C.

(Received June 3, 1998; Accepted October 20, 1998)

## ABSTRACT

Radiometric characteristics of the land surface nonlinearly depend on the surface state, so it is in general a great challenge to recover the surface state using mathematically-based schemes. Neural networks are known for their capability in dealing with nonlinear fittings. We investigate the use of a Dynamic Learning Neural Network (DLNN) in the retrieval of land surface parameters from radiometric signatures. Two case studies are considered. The first study is based on predictions from a 60-day summer dry-down simulation of the Land Surface Process/Radiobrightness (LSP/R) model, which manages land-air interactions and microwave radiative transfer in order to furnish temperature and moisture profiles of the vegetation and soil, and the corresponding brightness temperatures of the terrain. For the purpose of this investigation, the second study is based on LSP/R model predictions, which are used for model validation against a field campaign. Both cases utilize about 10% of the predictions from the LSP/R model to train the DLNN, and another 10% or so of the predictions as the ground truth to evaluate the DLNN retrievals. The training data include horizontally- and vertically-polarized brightnesses at 1.4, 19, and 37 GHz as the inputs of the DLNN, and the corresponding temperatures and moisture contents of the soil and canopy as the outputs. In the first study, we find that root mean square (rms) errors are less than 1% between DLNN retrievals and ground truth for all of the four surface parameters of interest. The rms errors are about 0.42 Kelvin for soil temperature (uppermost 5 mm), 0.11% for soil moisture (by volume), 0.034 Kelvin for canopy temperature, and 0.008 kg/m<sup>2</sup>. In the second study, the rms errors are slightly greater but within a reasonable range of less than 2% for all of four parameters.

**Key Words:** soil moisture, land surface process, radiobrightness, neural network

## 1. Introduction

Land and air are coupled through exchanges of moisture and energy, which are important boundary conditions of atmospheric circulation models (Smith *et al.*, 1994; Liang *et al.*, 1994). Land-surface parameters govern these exchanges through their dominance on the partitioning of incoming insolation into latent and sensible heat. These parameters include the temperatures and moisture contents of the soil and canopy. Among them, soil moisture is most important. Since soil moisture is highly variable in spatial and temporal domains (Bell *et al.*, 1980), observations of its distribution must be made constantly to maintain good quality of products from numerical weather prediction models. The remote sensing technique seems to be the only

solution.

Thermal infrared (TIR) remote sensing represents one way of detecting soil moisture and surface energy fluxes from space. In general, multispectral measurements from aircraft and satellite platforms are used to relate surface radiant temperature and vegetation fraction to surface wetness and energy fluxes (Price, 1990; Moran *et al.*, 1994; Diak *et al.*, 1995; Carlson *et al.*, 1995; Gillies and Carlson, 1995; Gilles *et al.*, 1997). This approach performs poorly during cloudy and rainy events, and over vegetated areas because the propagation path tends to become opaque to TIR signals.

Microwave remote sensing provides the second way to measure soil moisture from space. Compared with TIR, microwaves are capable of penetrating clouds and to some extent, rain and vegetation (Ulaby *et al.*,

1981). Many studies have been conducted to investigate retrievals of soil moisture using microwaves over the past two decades (Schmugge *et al.*, 1986; Jackson and Schmugge, 1989; Ahmed, 1995; Wigneron *et al.*, 1995). Retrievals are possible when they primarily rely on the sensitivity of brightness temperatures to soil moisture. Nevertheless, the highly nonlinear relationship between soil moisture and radiometric observations makes it less feasible to infer the former from the latter using a mathematically-based method.

Neural networks are well-known for their capability in solving nonlinear mappings. For example, they have been used in a broad range of studies, such as in monitoring rainfall (Xiao and Chandrasekar, 1997), clouds (Bankert and Aha, 1996), tornados (Marzban and Stumpf, 1996), ship waves (Fitch *et al.*, 1991), snow parameters (Tsang *et al.*, 1992), surface winds speeds (Thiria *et al.*, 1993; Stogryn *et al.*, 1994; Krasnopolsky *et al.*, 1995; Chen *et al.*, 1999), relative humidity (Cabrera-Mercader and Staelin, 1995), and forest change (Gopal and Woodcock, 1996), in (actively) retrieving surface parameters (Chen *et al.*, 1995), and in conducting image classification (Kanellopoulos *et al.*, 1992; Bischof *et al.*, 1992; Hara *et al.*, 1994). Recently, we demonstrated a neural network approach (Liou *et al.*, 1999a) that, based on dry-down simulations of the Land Surface Process/Radiobrightness (LSP/R) model, the L-band brightness temperature had an impact on radiometric sensing of land surface parameters over a prairie grassland. In this paper, we further investigate the neural approach by using more realistically radiometric signatures of the terrain to infer land surface parameters for practical use.

## II. The LSP/R Model and Its Validation

The LSP/R model consists of two modules, an LSP module and an R module. It was developed over a period of several years (Liou and England, 1996, 1998a, 1998b; Liou *et al.*, 1999b). The LSP module that treats energy and moisture exchanges between the land and atmosphere computes temperature and moisture profiles of the soil and canopy. Energy and moisture transfer in the soil and canopy involves solving the 1-dimensional form of the following coupled equations:

$$\frac{\partial X_{m,k}}{\partial t} = -\nabla \cdot \overline{Q}_{m,k} \quad (1)$$

$$\frac{\partial X_{h,k}}{\partial t} = -\nabla \cdot \overline{Q}_{h,k}, \quad (2)$$

where the subscript  $k$  represents the soil or canopy,  $X_m$  is the total water mass per unit volume,  $\text{kg/m}^3$ ,  $X_h$  is the total heat content per unit volume,  $\text{J/m}^3$ ,  $t$  is the time, s,  $\overline{Q}_m$  is the vector moisture (vapor and liquid) flux density,  $\text{kg/m}^2\text{-s}$ , and  $\overline{Q}_h$  is the vector heat flux density,  $\text{J/m}^2\text{-s}$ . At the land-air interface, heat flux includes components of radiant heat, sensible and latent heat, and heat exchanges due to rainfall. Moisture flux accounts for transfer due to evaporation and transpiration, and to precipitation and run-off. Within the soil, heat conduction, transfer of latent heat by means of vapor movement, and transfer of sensible heat in vapor and liquid comprises the total heat flux, and liquid and vapor flux densities account for the total moisture flux density. These fluxes include the effect of transpiration on the moisture flux and on the energy flux within the root zone. Many of the parameters that govern moisture and energy transfer are functions of the temperature and liquid water content of the soil and canopy. The nonlinear constitutive relations, the boundary conditions and forcings, and the numerical solutions of temperature and moisture to Eqs. (1) and (2) were presented by Liou *et al.* (1999b).

The R module manages radiative transfer within the canopy and absorption from the canopy to estimate terrain radiobrightness. The R module follows the approach of England and Galantowicz (1995). The combined soil and canopy radiobrightness is

$$Tb = T_{s,e}(1 - R_p(\mu))e^{-\tau_0/\mu} + T_{c,e}(1 - e^{-\tau_0/\mu})(1 + R_p(\mu)e^{-\tau_0/\mu}), \quad (3)$$

where  $T_{s,e}$  is the effective emitting temperature of the soil (Liou and England, 1996, 1998a),  $K$ ,  $R_p$  is the Fresnel reflectivity of the moist soil for polarization  $p$ ,  $\tau_0$  is the optical thickness of the canopy,  $\mu$  is the cosine of  $53^\circ$ , the incidence angle of Special Sensor Microwave/Imager (SSM/I), and  $T_{c,e}$  is the effective emitting temperature of the canopy,  $K$ .

A series of Radiobrightness Energy Balance Experiments (REBEX) were conducted to validate the LSP/R model (Kim and England, 1996a, 1996b; Galantowicz, 1995). REBEX-0 was conducted in a grass-covered research plot at the University of Michigan's Matthaei Botanical Gardens in Ann Arbor, MI, U.S.A., from August 19, 1992 to September 8, 1992 (Kim and England, 1996a). The soil at the site was a sandy loam, and the grass column density was from 3 to 3.8  $\text{kg/m}^2$ . REBEX-1 was a 7-month fall and winter experiment in grassland near Sioux Falls, South Dakota, during 1992-1993 (Galantowicz, 1995). The soil at the REBEX-1 site was a silty clay loam, and the grass column density was 3.7  $\text{kg/m}^2$ . REBEX-3 was a 1-year experiment in tussock tundra on the Alaskan North

**Table 1.** AD and SD Based upon Comparisons between Measured and Predicted Soil Temperatures at 2, 4, 8, 16, 32, and 64 cm Depths, Heat Flux at a 2 cm Depth, and Brightnesses at 19.35 GHz

Parameters	AD	SD
Canopy Temp, K	1.1	1.9
Soil Temp at 2 cm, K	1.9	2.1
Soil Temp at 4 cm, K	1.8	2.0
Soil Temp at 8 cm, K	1.6	1.7
Soil Temp at 16 cm, K	1.3	1.5
Soil Temp at 32 cm, K	1.1	1.2
Soil Temp at 64 cm, K	0.6	0.8
Heat Flux at 2 cm, W/m <sup>2</sup>	4.6	6.9
$Tb_s$ at 19.35 GHz, K	-0.06	1.1

Slope during 1994-1995 (Kim and England, 1996b). REBEX-4, a joint project with the Atmospheric Environment Service of Canada, was a 4-month growing season experiment in grass and bare soil at the REBEX-1 site during the summer of 1996.

We have validated the LSP/R model by forcing the model with observed weather and down-welling radiation during REBEX-1 and comparing model predictions of temperatures, heat flux, and radiobrightness with the corresponding REBEX-1 observations (Liou *et al.*, 1999b). Observations of a 14-day period from day 287 to day 300 of REBEX-1 were used in the validation. During the period, the grass was green and there was no snow cover. The average of the differences (AD) between the model predictions and REBEX-1 observations, and the corresponding standard deviations (SD) are listed in Table 1. In general, the model predictions agree with the corresponding measured values very well.

### III. The Dynamic Learning Neural Network (DLNN)

DLNN is utilized to manage a nonlinear mapping relation between the radiobrightnesses and the surface parameters. Based on a polynomial basis function expansion, a multilayer perceptron network is modified so that at the output layer, the functional form is linearized while the hidden layers remain nonlinear. The weighting functions in each layer are cascaded to form a long vector, through which the outputs and inputs are related (Tzeng *et al.*, 1994), i.e.,

$$y=Wx, \quad (4)$$

where the output vector  $y$  contains all the output nodes of a network, the long input vector  $x$  is formed by

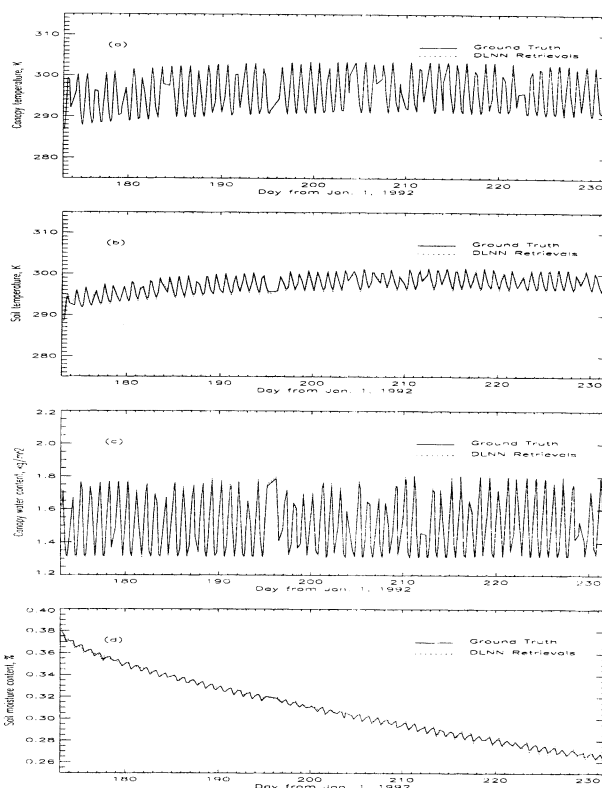


**Fig. 1.** (a) Canopy temperature, (b) soil temperature, (c) canopy water content, and (d) soil moisture content from ground truth and from DLNN retrievals.

concatenating all the input and hidden nodes in the network, and the long output weight matrix  $W$  is formed by concatenating all the weights that connected to each output node. This modification allows us to apply the dynamic Kalman filtering algorithm (Brown and Hwang, 1983) to adjust the network weights with a recursive minimum least square error, which is very suitable for computer implementation (Haykin, 1994). The network, i.e., the DLNN, bears features such as fast learning and built-in optimization of a weighting function at little expense of computer storage. The fast learning feature stems from the fact that updating of the weights is accomplished in a global manner while avoiding back-propagation, which usually makes the learning process very lengthy. DLNN was presented by Tzeng *et al.* (1994).

### IV. Simulations and Retrievals

Two case studies were conducted to evaluate the feasibility of retrieving surface parameters from radiobrightnesses using DLNN trained by the LSP/R model. Results from the first study (dry-down simulation) are shown in Fig. 1: (1) canopy temperature,

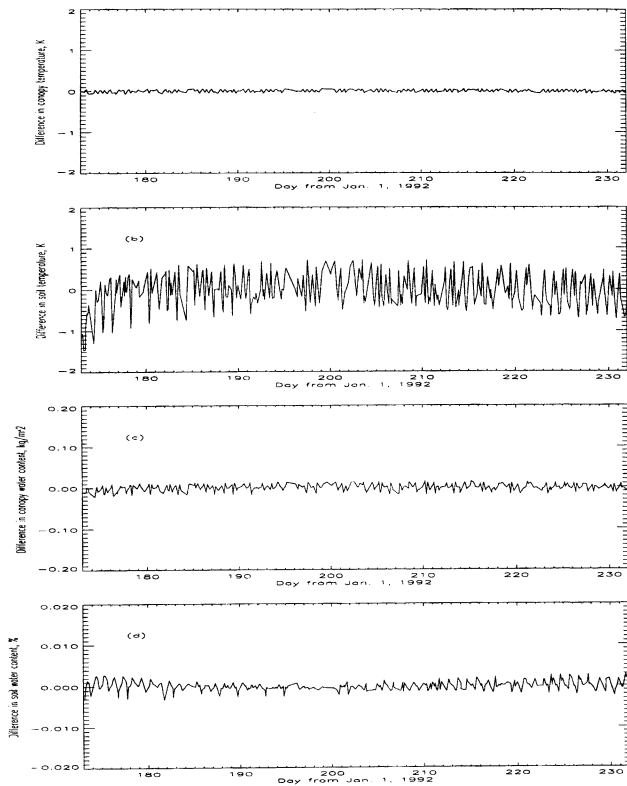


**Fig. 2.** Differences in (a) canopy temperature, (b) soil temperature, (c) canopy water content, and (d) soil moisture content between DLNN retrievals and the corresponding ground truth.

(2) soil temperature, (3) canopy water content, and (4) soil moisture content from ground truth and from DLNN retrievals. In general, the retrievals fit the ground truth very well. For example, it is obvious that there are no observable discrepancies between the retrieved canopy temperature and the corresponding reference.

Figure 2 shows the differences in (1) canopy temperature, (2) soil temperature, (3) canopy water content, and (4) soil moisture content between DLNN retrievals and ground truth. We find that the maximum differences between DLNN retrievals and ground truth are 0.07 Kelvin for canopy temperature, 1.5 Kelvins for soil temperature (uppermost 5 mm), 0.02 kg/m<sup>2</sup> for canopy water content, and 0.3% for soil moisture content. The corresponding rms errors are 0.034 Kelvin for canopy temperature, 0.42 Kelvin for soil temperature, 0.008 kg/m<sup>2</sup> for canopy water content, and 0.11% for soil moisture content. That is, the DLNN retrievals are all more than 99% accurate.

Results from the second study (field campaign) are shown in Fig. 3: (1) canopy temperature, (2) soil temperature, (3) canopy water content, and (4) soil moisture content from ground truth and from DLNN retrievals. The DLNN retrievals generally mimic the

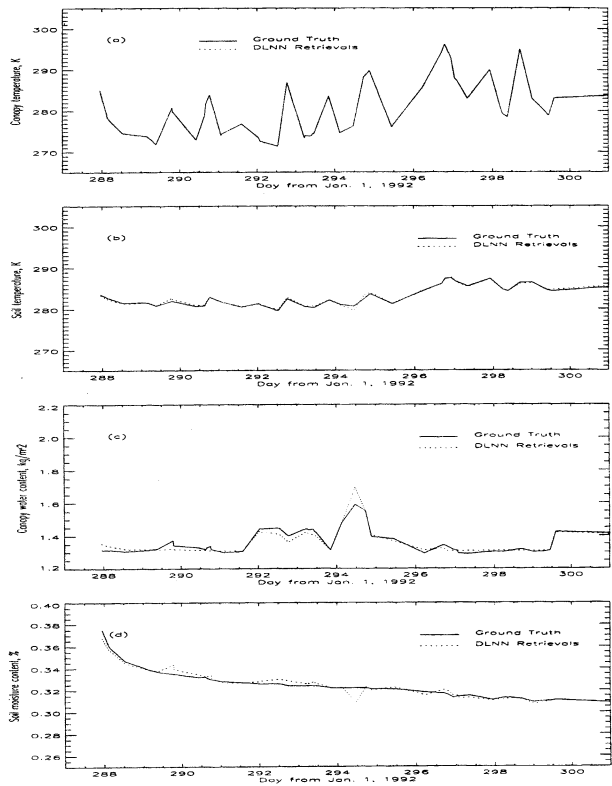


**Fig. 3.** (a) Canopy temperature, (b) soil temperature, (c) canopy water content, and (d) soil moisture content from ground truth and from DLNN retrievals.

ground truth considerably well. As shown in Fig. 4, differences between the retrievals and corresponding ground truth are small – less than 0.1 Kelvin for canopy temperature, less than 1.0 Kelvin for soil temperature (uppermost 5 mm), less than 0.1 kg/m<sup>2</sup> for canopy water content, and less than 1.3 % for soil moisture content. The corresponding rms errors are 0.025 Kelvin for canopy temperature, 0.29 Kelvin for soil temperature, 0.024 kg/m<sup>2</sup> for canopy water content, and 0.32% for soil moisture content. That is, the DLNN retrievals are all more than 98% accurate.

As shown in Fig. 3, the inferred canopy temperatures appear to match the corresponding ground truth better than do the other three parameters. Our interpretation includes three observations: (1) emissions at 19 and 37 GHz are primarily from the canopy – more than approximately 90% for the former and 95% for the latter (Liou *et al.*, 1999b); (2) brightnesses at 19 and 37 GHz are almost linearly related to the physical temperature of the canopy; and (3) brightnesses at 1.4, 19, and 37 GHz depend on the canopy moisture, soil temperature and moisture content with a higher degree of nonlinearity than they do on the canopy temperature. The total effect of 1 to 3 permits DLNN

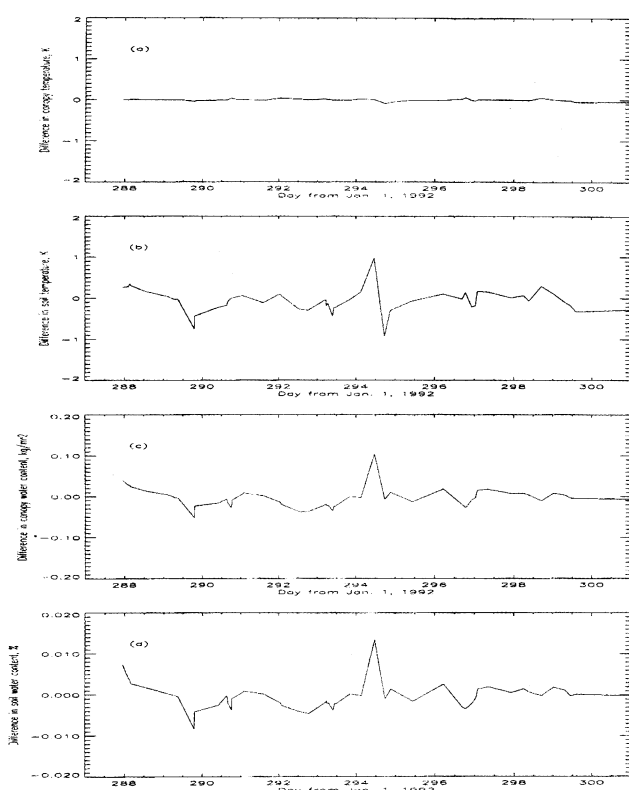


Fig. 4. Differences in (a) canopy temperature, (b) soil temperature, (c) canopy water content, and (d) soil moisture content between DLNN retrievals and the corresponding ground truth.

to infer the canopy temperature better than the other three parameters.

## V. Discussion and Conclusions

This paper has demonstrated that DLNN infers the surface parameters from radiobrightnesses relatively well. This implies that DLNN is capable of resolving the nonlinear relationships between surface parameters and radiobrightnesses. In addition, most of the uncertainties or errors produced in the retrieving process may primarily be from the training data. Hence, if one is using a reliable LSP/R model to provide a complete data set, the proposed retrieval approach can be very powerful.

Further study in two directions will be valuable. They are improvement and validation of the LSP/R model, and with the issue of how to properly utilize neural networks. The former would permit the LSP/R model to simulate a wider range of problems that are more likely to occur in reality. The latter would aim to effectively implement neural networks to deal with problems of interest based upon their characteristics. For example, DLNN may not be the best

candidate for solving problems with characteristics that are not clearcut or clearly defined, like the problem recently noted concerning the effect of scaling on the interpretability of mixed pixel radiobrightnesses (Liou *et al.*, 1998). It was found that 19.35 GHz brightnesses contain information about the canopy column density and its spatial variability in a sub-pixel. We are investigating the use of a Fuzzy DLNN to retrieve such information.

## Acknowledgment

This work has been supported by the NSC, R.O.C., under grants NSC 86-2111-M-008-035-T and NSC 87-2111-M-008-021.

## References

- Ahmed, N. U. (1995) Estimating soil moisture from 6.6 GHz dual polarization, and/or satellite derived vegetation index. *Int. J. Remote Sensing*, **16**, 687-708.
- Bankert, R. L. and D. W. Aha (1996) Improvement to a neural network cloud classifier. *J. Appl. Meteorol.*, **35**, 2036-2039.
- Bell, K. R., B. J. Blanchard, T. J. Schmugge, and M. W. Witzak (1980) Analysis of surface moisture variations within large-field sites. *Water Resour. Res.*, **16**, 796-810.
- Bischof, H., W. Schneider, and A. J. Pinz (1992) Multispectral classification of Landsat images using neural networks. *IEEE Trans. Geosci. Remote Sensing*, **30**, 482-489.
- Brown, R. G. and P. Y. C. Hwang (1983) *Introduction to Random Signals and Applied Kalman Filtering*, 2nd Ed. Wiley, New York, NY, U.S.A.
- Cabrera-Mercader, C. R. and D. H. Staelin (1995) Passive microwave relative humidity retrievals using feedforward neural networks. *IEEE Trans. Geosci. Remote Sensing*, **33**, 1324-1328.
- Carlson, T. N., R. R. Gillies, and T. J. Schmugge (1995) An interpretation of water content and fractional vegetation cover. *Agric. Meteorol.*, **77**, 191-205.
- Chen, K. S., W. L. Kao, and Y. C. Tzeng (1995) Retrieval of surface parameters using dynamic learning neural network. *Int. J. Remote Sensing*, **16**, 801-809.
- Chen, K. S., Y. C. Tzeng, and P. T. Chen (1999) Retrieval of ocean winds from satellite scatterometer by a neural network. *IEEE Trans. Geosci. Remote Sensing*, **37**, 247-256.
- Diak, G. R., R. M. Rabin, K. P. Gallo, and C. M. U. Neale (1995) Regional-scale comparisons of vegetation and soil wetness with surface energy properties from satellite and in-situ observations. *Remote Sens. Rev.*, **12**, 355-382.
- England, A. W. and J. F. Galantowicz (1995) Observed and modeled radiobrightness of prairie grass in early fall. 1995 IEEE Int'l Geosci. Remote Sensing Symp., Florence, Italy.
- Fitch, J. P., S. K. Lehman, F. U. Dowla, S. Y. Lu, E. M. Johanson, and D. M. Goodman (1991) Ship wave detection procedure using conjugate gradient trained neural network. *IEEE Trans. Geosci. Remote Sensing*, **29**, 718-726.
- Galantowicz, J. F. (1995) *Field Data Report for the First Radiobrightness Energy Balance Experiment (REBEX-1), October 1992-April 1993, Sioux Falls, South Dakota*. Technical Report RL-913, UM Radiation Laboratory, Ann Arbor, MI, U.S.A.
- Gillies, R. R. and T. N. Carlson (1995) Thermal remote sensing of surface soil water content with partial vegetation cover for incorporation into climate models. *J. Appl. Meteorol.*, **34**, 745-

756.

- Gillies, R. R., J. Cui, T. N. Carlson, W. P. Kustas, and K. S. Humes (1997) Verification of a method for obtaining surface soil water content and energy fluxes from remote measurements of NDVI and surface radiant temperature. *Int. J. Remote Sens.* (in press).
- Gopal, S. and C. Woodcock (1996) Remote sensing of forest change using artificial neural networks. *IEEE Trans. Geosci. Remote Sensing*, **34**, 398-404.
- Hara, Y., R. G. Atkins, S. H. Yueh, R. T. Shin, and J. A. Kong (1994) Application of neural networks to radar image classification. *IEEE Trans. Geosci. Remote Sensing*, **32**, 100-109.
- Haykin, S. (1994) *Neural Networks*. Prentice-Hall, Englewood Cliffs, NJ, U.S.A.
- Jackson, T. J. and T. J. Schmugge (1989) Passive microwave remote sensing system for soil moisture: some supporting research. *IEEE Trans. Geosci. Rem. Sen.*, **GE-27**, 225-235.
- Kanellopoulos, A., A. Varfis, G. G. Wilkinson, and J. Megier (1992) Land-cover discrimination in SPOT HRV imagery using an artificial neural network—a 20-class experiment. *Int. J. Remote Sensing*, **13**, 917-924.
- Kim, E. J. and A. W. England (1996a) *Field Data Report for Radiobrightness Energy Balance Experiment 0 (REBEX-0), August, 1992-September, 1993: UM Matthaei Botanical Gardens*. Technical Report RL-916, UM Radiation Laboratory, Ann Arbor, MI, U.S.A.
- Kim, E. J. and A. W. England (1996b) *Field Data Report for the Third Radiobrightness Energy Balance Experiment (REBEX-3), September 1994 – September 1995, Wet Acidic Tundra on the Alaskan North Slope*. Technical Report RL-918, UM Radiation Laboratory, Ann Arbor, MI, U.S.A.
- Krasnopolsky, V. M., L. C. Breaker, and W. H. Gemmill (1995) A neural network as a nonlinear transfer function model for retrieving surface wind speeds from the special sensor microwave imager. *J. Geophys. Res.*, **100**, 11033-11045.
- Liang, X., D. P. Lettenmaier, E. F. Wood, and S. J. Burges (1994) A simple hydrologically based model of land surface water and energy fluxes for general circulation models. *J. Geophys. Res.*, **99**, 14415-14428.
- Liou, Y. A. and A. W. England (1996) Annual temperature and radiobrightness signatures for bare soils. *IEEE Trans. Geosci. Remote Sensing*, **34**, 981-990.
- Liou, Y. A. and A. W. England (1998a) A land surface process/radiobrightness model with coupled heat and moisture transport in soil. *IEEE Trans. Geosci. Remote Sensing*, **36**, 273-286.
- Liou, Y. A. and A. W. England (1998b) A land surface process/radiobrightness model with coupled heat and moisture transport for freezing soils. *IEEE Trans. Geosci. Remote Sensing*, **36**, 669-677.
- Liou, Y. A., E. J. Kim, and A. W. England (1998) Radiobrightness of prairie soil and grassland during dry-down simulations. *Radio Sci.*, **33**, 259-265.
- Liou, Y. A., Y. C. Tzeng, and K. S. Chen (1999a) A neural network approach to radiometric sensing of land surface parameters. *IEEE Trans. Geosci. Remote Sensing* (in press).
- Liou, Y. A., J. Galantowicz, and A. W. England (1999b) A land surface process/radiobrightness model with coupled heat and moisture transport for prairie grassland. *IEEE Trans. Geosci. Remote Sensing* (in press).
- Marzban, C. and G. J. Stumpf (1996) Neural network for tornado prediction based on Doppler radar-derived attributes. *J. Appl. Meteorol.*, **35**, 617-626.
- Moran, M. S., T. R. Clarke, Y. Inoue, and A. Vidal (1994) Estimating crop water deficit using the relation between surface-air temperature and spectral vegetation index. *Remote Sens. Environ.*, **49**, 246-263.
- Price, J. C. (1990) Using spatial context in satellite data to infer regional scale evapotranspiration. *IEEE Trans. Geosci. Remote Sens.*, **28**, 940-948.
- Schmugge, T. J., P. E. O'Neill, and J. R. Wang (1986) Passive microwave soil moisture research. *IEEE Trans. Geosci. Rem. Sen.*, **GE-24**, 12-22.
- Smith, C. B., M. N. Lakhtakia, W. J. Capehart, and T. N. Carlson (1994) Initialization of soil-water content in regional-scale atmospheric prediction models. *Bull. Amer. Meteor. Soc.*, **75**, 585-593.
- Stogryn, A. P., C. T. Butler, and T. J. Bartolac (1994) Ocean surface wind retrievals from special sensor microwave imager data with neural networks. *J. Geophys. Res.*, **99**, 981-984.
- Thiria, S., C. Mejia, F. Badran, and M. Crepon (1993) A neural network approach for modeling nonlinear transfer functions: application for wind retrieval from spaceborn scatterometer data. *J. Geophys. Res.*, **98**, 22827-22847.
- Tsang, L., Z. Chen, S. Oh, R. J. Marks, II, and A. T. C. Chang (1992) Inversion of snow parameters from passive microwave remote sensing measurement by a neural network trained with a multiple scattering model. *IEEE Trans. Geosci. Remote Sensing*, **30**, 1015-1024.
- Tzeng, Y. C., K. S. Chen, W. L. Kao, and A. K. Fung (1994) A dynamic learning neural network for remote sensing applications. *IEEE Trans. on Geosci. and Remote Sensing*, **32**, 1096-1102.
- Ulaby, F. T., R. K. Moore, and A. K. Fung (1981) *Microwave Remote Sensing, Active and Passive*, Vol. I. Artech House, Norwood, MA, U.S.A.
- Wigneron, J. P., A. Chanzy, J. C. Calvet, and N. Bruguier (1995) A simple algorithm to retrieve soil moisture and vegetation biomass using passive microwave measurements over crop fields. *Remote Sens. Environ.*, **51**, 331-341.
- Xiao, R. and V. Chandrasekar (1997) Development of a neural network based algorithm for rainfall estimation from radar observations. *IEEE Trans. Geosci. Remote Sens.*, **35**, 160-172.

## 應用類神經網路於輻射計量地表參數之研究

劉說安\* 曾裕強\*\* 陳錕山\*

\*國立中央大學太空及遙測研究中心

\*\*國立聯合工商專科學校電子工程科

### 摘 要

地表輻射計量特性非線性地依賴其呈現狀態，因此，一般而言，利用植基於數學理論去推演這些狀態的方法，必須面臨極大的挑戰。類神經網路以善於解決非線性問題聞名，本文探討應用動態學習類神經網路(Dynamic Learning Neural Network; DLNN)於輻射計量地表參數之研究，共討論兩種個案。第一個個案根據一個地表過程／亮溫(Land Surface Process/Radiobrightness; LSP/R)模式在夏季中60天乾燥模擬結果。LSP/R模式處理地表與大氣間交互作用及微波輻射傳送，估計植物與土壤的溫濕剖面及地表亮溫。為了實用性，第二個個案根據驗證LSP/R模式的模擬資料。兩種個案中，大約百分之十的模擬資料用來訓練DLNN，另外約百分之十的資料當作“地真”(ground truth)來評估DLNN反演值。訓練資料包含1.4，19及37 GHz垂直與水平亮溫當作DLNN的輸入，以及相對應植物與土壤的溫濕參數當作輸出。我們發現，在第一個個案中，四種DLNN反演之植物及土壤的溫濕參數值與地真間均方根差都小於1%，其中，對於土壤溫度（最上5 mm）為0.42 K，對於土壤含水率（體積比）為0.11%，對於植物溫度為0.034 K，對於植物含水率為0.008 kg/m<sup>2</sup>。在第二個個案中，四種均方根差略微增加，然而都在一個小於2%的合理範圍內。